Electronic Supplementary Material (ESI) for ChemComm.

SUPPLEMENTARY INFORMATION

Intramolecular rotations and electronic states of iron in the iron bis(dicarbollide) complex $Fe[(C_2B_9H_{11})_2]$ studied by a ^{57}Fe nuclear probe and computational methods

K. Bednarska-Szczepaniak,[a] K. Dziedzic-Kocurek,[b] E. Przelazły,[a] J. Stanek [b] and Z. Leśnikowski [a]†

[a]*Laboratory of Medicinal Chemistry, Institute of Medical Biology PAS, Lodowa 106, 92-232 Łódź, Poland;*

[b]*Marian Smoluchowski Institute of Physics, Jagiellonian University, Prof. Stanisława Łojasiewicza 11, 30-345 Kraków, Poland.*

†*Corresponding author: Zbigniew J. Leśnikowski, zlesnikowski@cbm.pan.pl.*

1. Chemistry

Cesium salt of iron(III)bis(dicarbollide) (**1**) was purchased from Katchem Ltd. (Prague, Czech Republic), and it was additionally purified by silica gel column chromatography (230-400 mesh, Sigma-Aldrich, Steinheim, Germany) using a gradient of acetonitrile in methylene chloride from 0% to 30% as an eluting solvent system (purity > 99,9%). 8-Dioxane iron bis(dicarbollide) (**2**) was synthesized according to the literature procedure based on the reaction of 1,4-dioxane (also used as the reaction medium) in the presence of dimethyl sulfate $(CHO_3)_2SO_2$ [5. J. Plesek, B. Gruner, J. Machacek, I. Cisarova and J. Caslavsky, J. Organomet. Chem., 2007, 692, 4801].

2. Mössbauer spectroscopy measurements

The Mössbauer spectra of 25 mg powder samples of iron(III) bis(dicarbollide) (**1**) or 8-dioxane iron bis(dicarbollide) (**2**) (Fig. 2, Fig. SI 1) were recorded in routine transmission geometry between 68 and 300 K using a WissEl spectrometer (Wissenschaftliche Electronic GmbH, Ortenberg, Germany) with a bath cryostat. The temperature stabilization was better than 0.2 K. The reported spectra were numerically evaluated using the *WinNormos-for-Igor* package (Wissenschaftliche Electronic GmbH, Ortenberg, Germany).

3. Calculation methods

The density functional theory (DFT) method was applied to calculate charge distribution and the dipole moments, in **1** and **2**. Calculations were performed using *transoid* and *cisoid* congruent crystallographic structures of **1** and **2**, respectively, implemented from the Cambridge Crystallographic Data Centre (CCDC, https://www.ccdc.cam.ac.uk/structures), as CCDC 1172189 (**1**) and CCDC 647876 (**2**). To obtain better insight into the distribution of the electronic charge on **1** and **2**, as well as the electronic gradients in the molecules, calculations were performed using the PBE exchange-correlation functional and BP86 (designed for metallacarboranes), as well as B3-PW91 or B3-LYP hybrid functionals alternatively, with an Ahlrichs VDZ basis set. These methods provided insight into both structures **1** and **2**; the first structure had a net charge of -1, and the second structure was neutral. Since the DFT B3-PW91 or B3-LYP/Ahlrichs VDZ methods were not applicable for **2** bearing a hypothetical net negative charge of -1 suggested by the Mössbauer measurements, the extended basis set was applied (Table SI 1, Supplementary Information). The specific structure of the fesane-dioxane (**2**) severely restricts the use of DFT methods applied for unmodified metallacarboranes (using BP86 or PBE functionals). Whereas the best results for **1** were obtained with DFT/PBE, DFT/B3-LYP, and DFT/B3-PW91

methods, realistic charge distribution in **2** was obtained using hybrid functionals, B3-PW91 and B3-LYP, i.e. positive charge on Fe, electronegative C1, C2, C1', and C2', hydridic nature of H, positively charged dioxane moiety (in **2**). DFT BP86 method gave unrealistic high atomic charges in **2** (data not shown). Additionally, the DFT methods at PBE0/cc-pvtz and B3-PW91/cc-pvtz levels gave similar unequal charge distribution for **2** (dipole moments 4.55 and 4.68 D, respectively, data not shown). Nevertheless, the DFT methods using exchange-correlation functional PBE, or hybrid PBE0, although readily applied in metallacarborane calculations, gave unrealistic negative charge on Fe ion in **2** (-0.176, and -0.087, respectively). However, a similar charge distribution on the dioxane modifier, +0.325 – +0.398 was obtained for all calculation methods (Table SI 1). All calculations were performed with Hyperchem Professional 7 (Hypercube Inc., USA, Gainesville, FL) and Gaussian 16 Rev. A.03 software (Gaussian 16, Revision A.03, M. J. Frisch et. al., Gaussian, Inc., Wallingford CT, 2016).

4. Dynamics of the iron bis(dicarbollide) complexes 1 and 2.

The dynamics of iron ion may be concluded from Mössbauer spectra from temperature dependence of recoil free fraction, f, which is proportional to the area of the absorption lines in the spectrum:

$$f = \exp(-\frac{< x^2 > E_\gamma^2}{(\hbar c)^2}) \qquad (1)$$

where $<x^2>$ is the mean square displacement of ^{57}Fe nuclei and E_γ is the energy of the Mössbauer transition (14.4 keV) and from the thermal shift or second order Doppler shift, δ_{SOD},

$$\delta_{SOD} = -E_\gamma \frac{< v^2 >}{2c^2} \qquad (2)$$

where $<v^2>$ is the mean square velocity of ^{57}Fe nuclei.
Both, $<x^2>$ and $<v^2>$ may be expressed in term of "Mössbauer" Debye temperature of iron, Θ_D. From the fit of the temperature dependence of recoil free fraction to that model (solid lines in Fig. SI 4B), one obtains Θ_D = 189(5) K or 152(10). The decrease of the Debye temperature points out that dioxane addition softens the iron-carborane ligand bonds.

From the thermal shift analysis, one may obtain much less accurate values of Debye temperatures: Θ_D = 580(20) and 610(30) K for **1** and **2**, respectively (Fig. SI 4A). Such discrepancies, i.e., different values of Debye temperatures calculated from the temperature of the thermal shift and temperature dependence of the spectrum area, are often found, reflecting the fact that the Debye model of atomic vibrations is not adequate for molecular crystals.

The infra molecular dynamics may by concluded from the temperature dependence of the hyperfine interactions, here electric quadrupole interaction acting on ^{57}Fe nuclei, functioning as a sensor of the electric field gradient produced by its ligands. The establishment of the full electric field gradient tensor (EFG) is not feasible. Thus, we applied a simplified model in which the main axis of the axial EFG and its sign remained constant during rotation of dicarbollide groups.
The method of the simulation was adopted from Herta et al., where the dynamically induced temperature dependence of QS in oxymyoglobin was explained [16]. First, the time dependence of the amplitude of the absorption probability of gamma radiation, $I(t)$, on two nuclear levels separated by temperature-dependent quadrupole splitting, $QS(T)$, is calculated. Next, the absorption probability as a function of frequency, $|R(\omega)|^2$, is obtained, i.e., the absorption spectrum is calculated, where $R(\omega)$ is the Fourier transform of $I(t)$. The simulation was performed for frequencies of rotation, n, in units of $1/\tau$, between 0.01 and 100 (if n = 1, it means that the rotation period lasts 141 ns, and the corresponding frequency

reaches 7x10^6 Hz). Examples of the simulated *I*(*t*) and the expected spectra *R*(ω) are shown in Fig. SI 5. The simulated spectra were fitted by a Lorentzian doublet, i.e., in the same way as the experimental spectra. The simulated spectra deviate strongly from a Lorentzian shape, especially at higher temperatures. The same behavior was observed in the experimental spectra. The expected line width as a function of the rotation frequency is shown in the left panel of Fig. SI 6. The simulation method is related to the classical problem of rumbling sound waves produced by two tuning forks for which the difference in the frequencies is time dependent. Here, the amplitude of the sound wave and the spectrum of acoustic intensity are analogs of I(t) and R(ω), respectively. By comparison of the experimental line broadening at different temperatures in Fig. SI 4, with the simulated line broadening for different rotation frequencies in Fig. SI 6, one can relate the rotation frequency with the temperature, i.e., n(T) (Fig. SI 6, right panel). Using the Arrhenius relation and by fitting n(T) to the function:

$$n(T) = n_0 \exp\left(-\frac{E_\gamma}{kT}\right) \qquad (3)$$

we estimated the energy barrier for the rotation E_r = 24 meV (2.5 kJ/mol = 0.6 kcal/mol) and pre-exponential factor n_0 = 3.0 (ν_o= 2.7*10^7 Hz). Thus, the rotation frequency at 293 K is 1.0*10^7 Hz.

Table SI 1. Atomic charges of Fe, C, and hydridic H atoms in **1** and **2**, calculated on the basis of the density functional theory (DFT, PBE, B-PW91 and B3LYP functionals is for comparison). Endpoint total energy values (a.u.) are provided below. The numbering of atoms in **1** and **2** is shown below.

method	B3-PW91/Ahlrichs VDZ		B3-LYP/Ahlrichs VDZ		B3-LYP/Ahlrichs VTZ 6-311++G**/6-31G*	PBE/Ahlrichs VDZ	
Compound Net charge conformer	**1** -1 *transoid*	**2** 0 *cisoid*	**1** -1 *transoid*	**2** 0 *cisoid*	**2** -1 *cisoid*	**1** -1 *transoid*	**2** 0 *cisoid*
Fe	0.698	0.841	0.755	0.779	0.497	0.701	-0.176
C1	-0.723	-0.661	-0.665	-0.613	-0.789	-0.643	-0.528
C2	-0.724	-0.670	-0.662	-0.625	-0.545	-0.644	-0.456
C3	-0.714	-0.718	-0.665	-0.668	-0.786	-0.643	-0.537
C4	-0.714	-0.675	-0.662	-0.625	-0.660	-0.644	-0.627
Hydridic H	-0.020– -0.057	-0.027	-0.041– -0.105	-0.042	-0.004	-0.034– -0.092	0.020– -0.204
Charge cluster 1 (dioxane) cluster 2 difference[#]	-0.853 – -0.845 -	-0.116 (+0.329) -0.725 0.609	-0.877 – -0.878 -	-0.093 (+0.325) -0.686 0.593	-0.425 (+0.398) -1.074 0.649	-0.850 – -0.851 -	-0.055 (+0.352) -0.120 65
Dipole moment	–	4.80	–	4.56	n.a.	–	9.14
Total energy	-1876.06	2182.3	-1875.40	-2181.85	-2183.19	-1865.45	-2177.3

Atom numbering

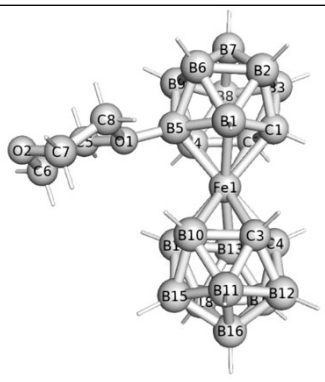

Calculations were performed for native crystal structures: CCDC 1172189 (**1**, *transoid*), CCDC 1585386 (**1**, *cisoid*), and CCDC 647876 (**2**); crystal structure data were downloaded from the Cambridge Structural Database (CSD): https://www.ccdc.cam.ac.uk/structures. UHF method was applied for all calculations; mixed basis sets was applied for **2** (net charge -1): Ahlrichs VDZ(Fe), 6-311++G**(ligand atoms adjacent to Fe), and 6-31G*(other atoms); n.a. – not applicable; [#]- the charge difference between two clusters (dioxane-modified and unmodified).

Table SI 2. Mössbauer parameters of the iron(III) bis(dicarbollide) (**1**) spectra; T: temperature, IS: isomer shift vs. metallic iron, QS: quadrupole splitting, W: line width, A: area, f: recoil free fraction.

T [K]	**IS [mm/s]**	**QS [mm/s]**	**W [mm/s]**	**A [mm/s]**	**f**
68	0.267	1.301(4)	0.365(7)	0.03800(64)	0.735
80	0.258	1.314(1)	0.380(2)	0.04133(17)	0.705
90	0.262	1.312(2)	0.397(2)	0.03590(21)	0.682
100	0.260	1.302(4)	0.415(7)	0.03457(5)	0.659
120	0.255	1.297(2)	0.472(4)	0.03225(4)	0.614
150	0.242	1.281(2)	0.591(4)	0.02845(18)	0.551
170	0.243(6)	1.276(10)	0.696(19)	0.02733(72)	0.512
190	0.227	1.249(6)	0.755(11)	0.02415(34)	0.476
210	0.216	1.223(5)	0.789(9)	0.02227(24)	0.442
230	0.215(40)	1.256(21)	0.789(40)(?)	0.0210(11)	0.410
273	0.189	1.255(6)	0.643(10)	0.01824(3)	0.349
293	0.173	1.266(3)	0.586(5)	0.01683(15)	0.324
310	0.163(3)	1.254(3)	0.550(9)	0.01541(2)	0.304

Table SI 3. Mössbauer parameters of the 8-dioxane iron bis(dicarbollide) (**2**) spectra; T: temperature, IS: isomer shift vs. metallic iron, QS: quadrupole splitting, W: line width, A: area, f: recoil free fraction.

T [K]	**IS [mm/s]**	**QS [mm/s]**	**W [mm/s]**	**A [mm/s]**	**f**
80	0.241	0.626	0.668	0.04998	0.597
100	0.239	0.62	0.718	0.04351	0.535
150	0.237	0.564	0.921	0.02908	0.403
200	0.241	0.535	0.949	0.02325	0.303
250	0.175	0.494	0.742	0.01258	0.226
293	0.154	0.489	0.598	0.01119	0.176

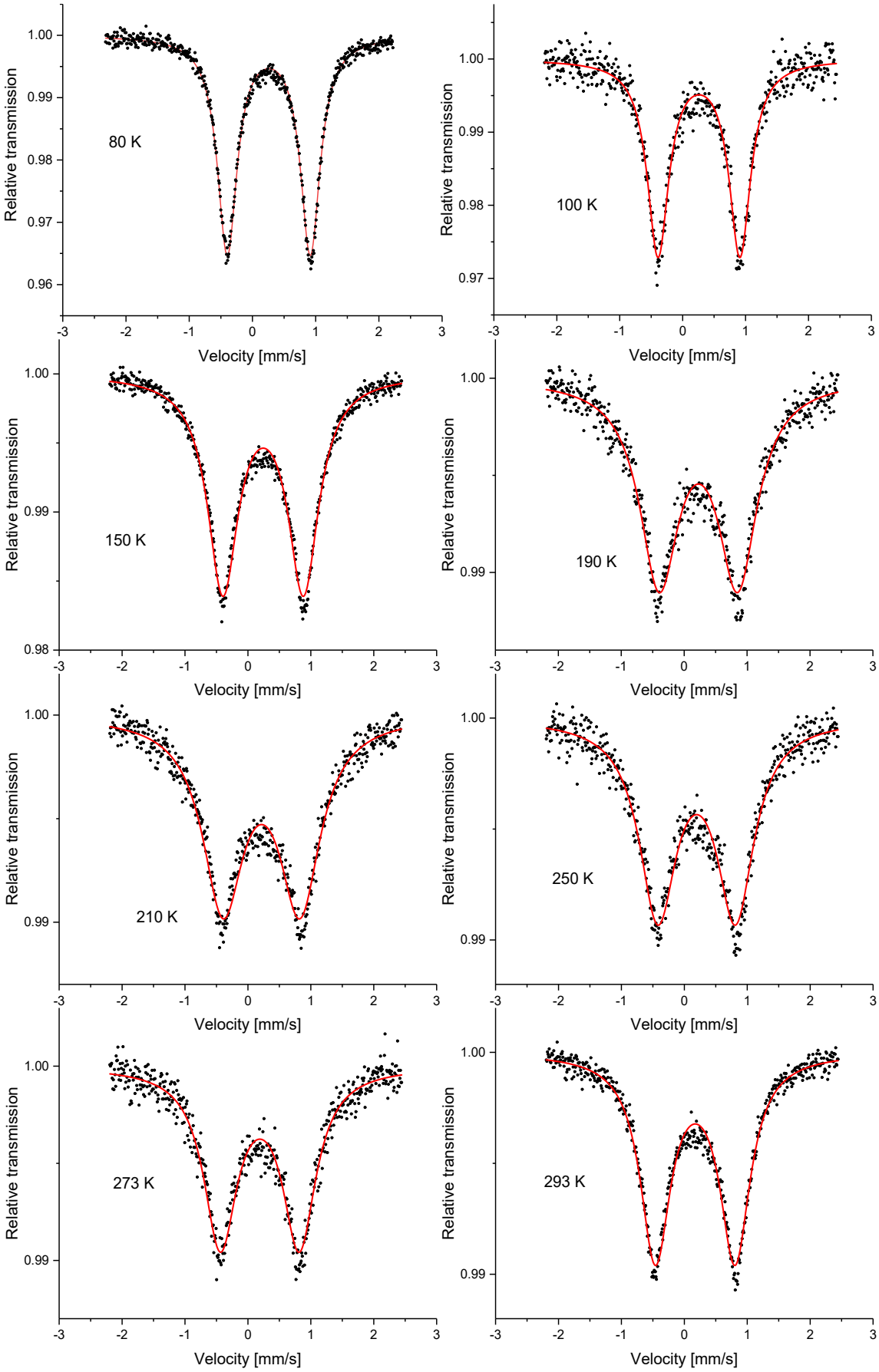

Figure SI 1. Mössbauer spectra of iron(III) bis(dicarbollide) (1) at temperatures as marked.

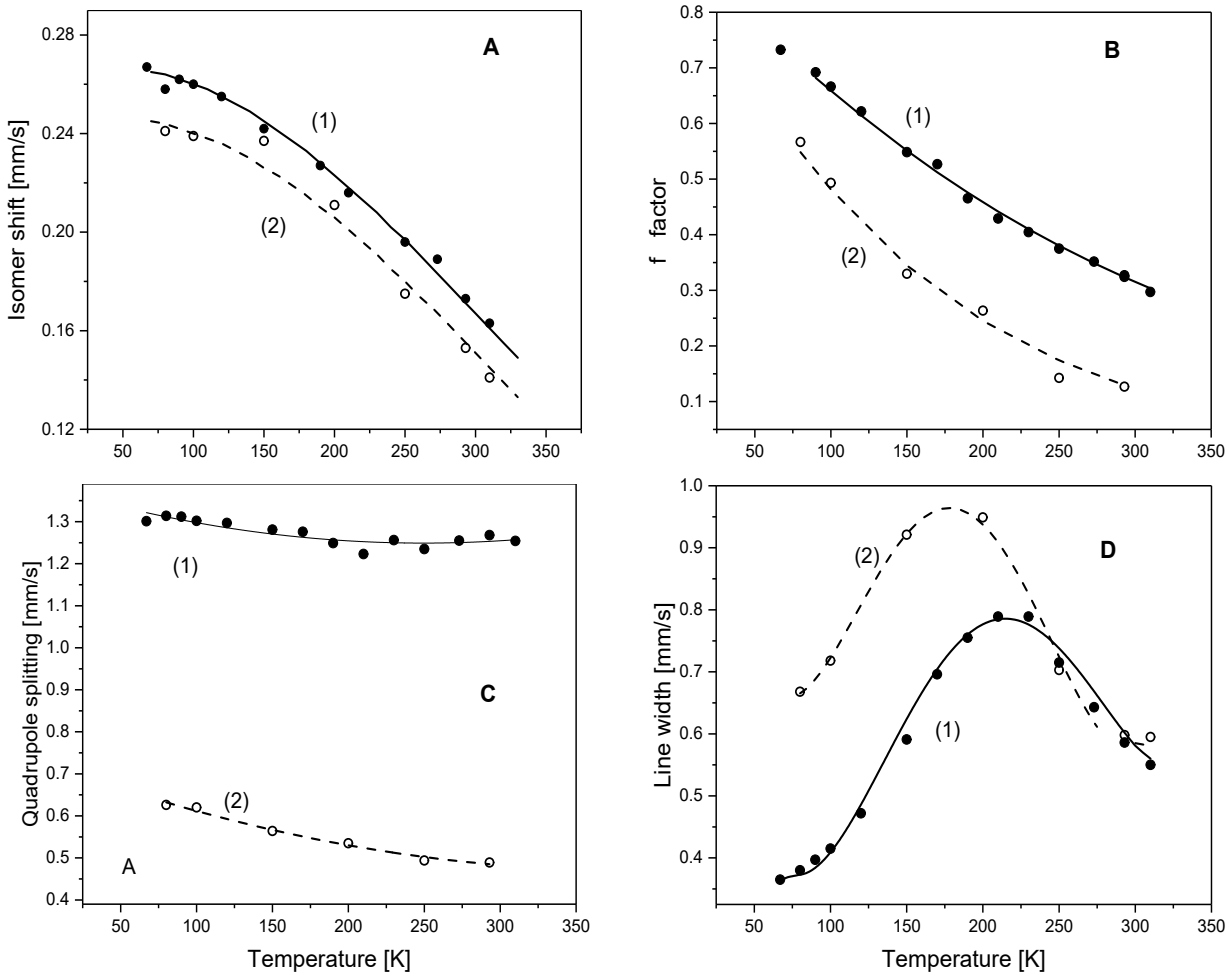

Figure SI 2. Temperature dependence of the isomer shift (A), recoil free fraction (f factor) calculated from the spectrum area (B), quadrupole splitting (C), and line width (D) of iron(III) bis(dicarbollide) (**1**, full dots) and 8-dioxane iron bis(dicarbollide) (**2**, open dots). In A and B, lines are the fits to the Debye model, and in C and D, lines are the polynomial fits.

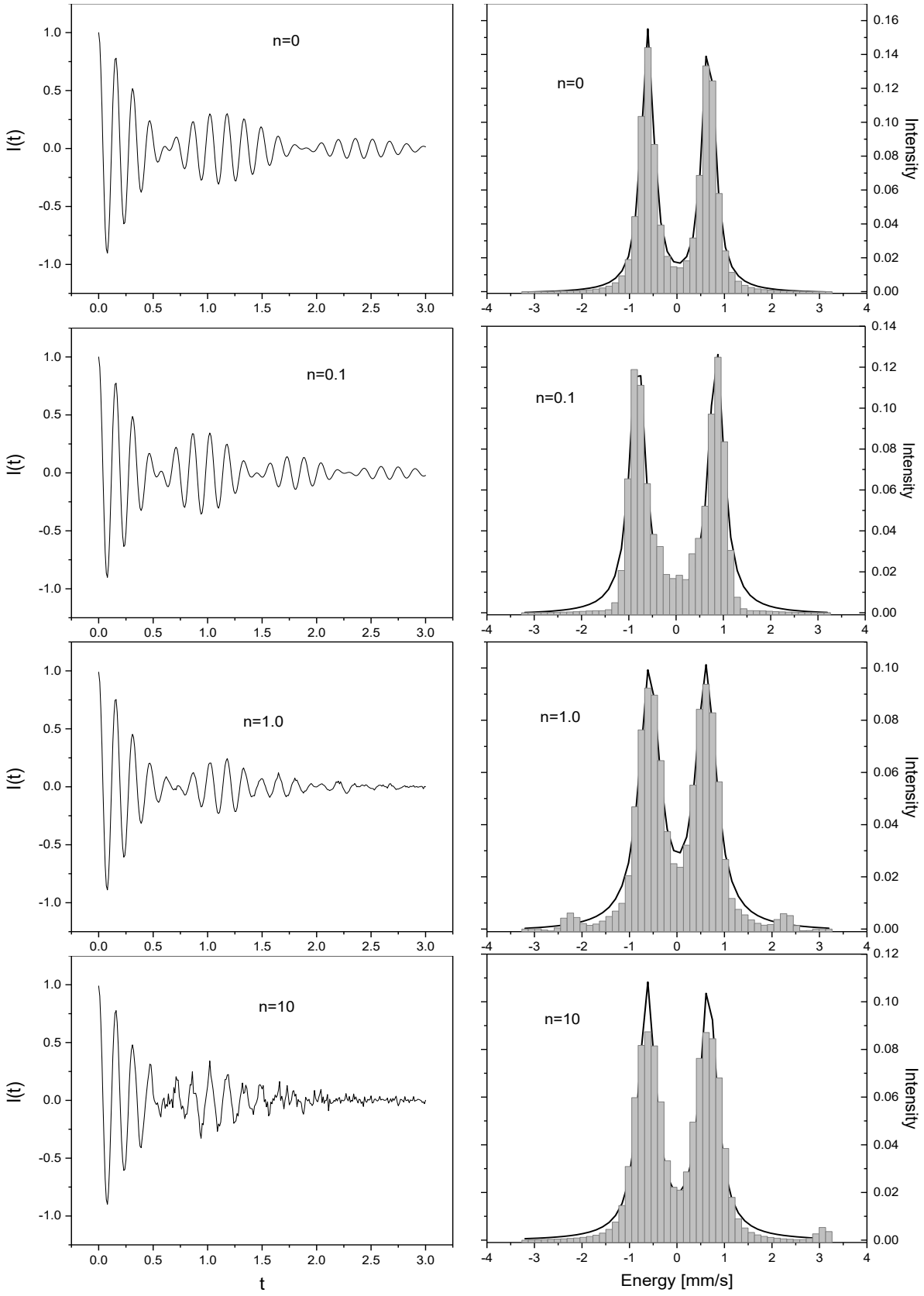

Figure SI 3. First column: simulated time dependent amplitude of absorption probability for different rotation frequencies (in $1/\tau$ units, τ =141 ns). Second column: normalized simulated spectra fitted with Lorentzian doublets, solid line.

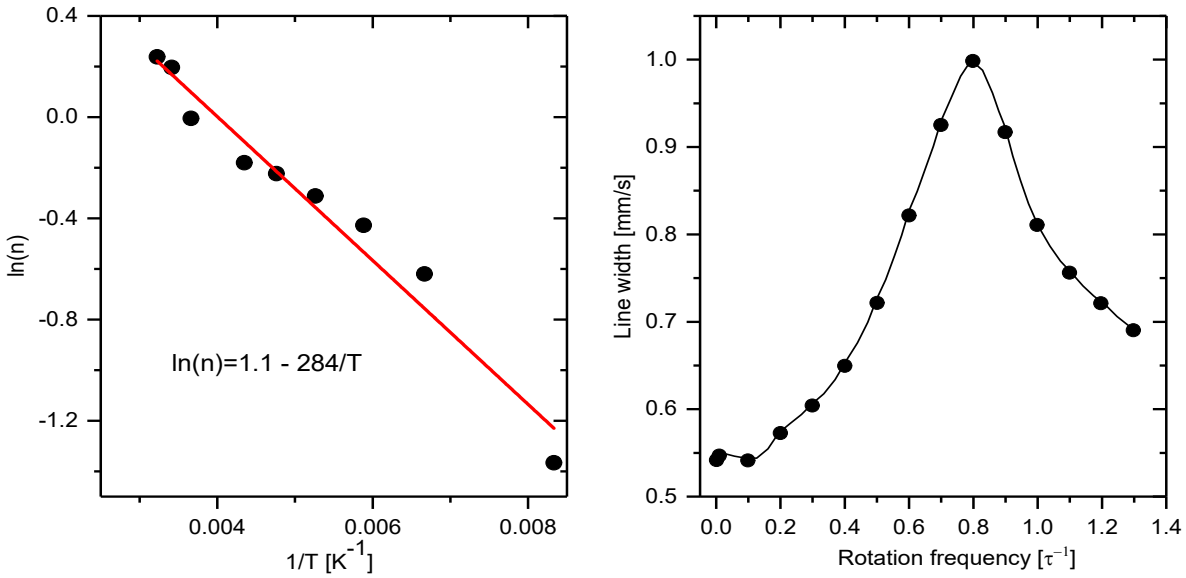

Figure SI 4. Left panel - Arrhenius plot of the rotation frequency as function of temperature; right panel - relative broadening of the simulated absorption lines as function of the rotation frequencies.